Coulomb-corrected quantum trajectories in strong-field ionization

S. V. Popruzhenko
Max-Planck-Institut für Kernphysik, Postfach 103980, 69029 Heidelberg, Germany
and Moscow State Engineering Physics Institute, Kashirskoe Shosse 31, 115409, Moscow, Russia

G. G. Paulus
Institute of Optics and Quantum Electronics, Friedrich Schiller University of Jena, Max-Wien-Platz 1, 07743 Jena, Germany
and Department of Physics, Texas A&M University, College Station, Texas 77843, USA

D. Bauer
Max-Planck-Institut für Kernphysik, Postfach 103980, 69029 Heidelberg, Germany
(Received 26 November 2007; published 20 May 2008)

Nonperturbative analytical quantum treatments of strong-field laser-atom interaction are essentially based on the assumption that binding forces are negligible once the electron is emitted because the further dynamics are considered as being dominated by the laser field. In this work we introduce a Coulomb-corrected strong-field theory of photoionization based on quantum trajectories and show how binding forces lead to strong qualitative effects in above-threshold ionization of atoms. We examine the theory by comparing experimental data for elliptically polarized laser fields and results from the *ab initio* solution of the time-dependent Schrödinger equation with our theoretical predictions. The comparison shows good quantitative agreement with the *ab initio* results and reasonable agreement with the data. For ground states with nonzero angular momentum we show a strong circular dichroism in the high-energy (rescattering) part of photoelectron spectra.

DOI: 10.1103/PhysRevA.77.053409 PACS number(s): 32.80.Rm, 03.65.Sq, 31.15.A−

I. INTRODUCTION

Impressive progress has been achieved in strong-field laser physics during the past years, including the introduction of new experimental techniques such as the reaction microscope [1], new kinds of laser sources such as phase-stabilized few-cycle pulses [2], and generation of attosecond soft x-ray pulses [3]. Nonperturbative descriptions of intense laser-atom interaction are commonly based on the strong-field approximation (SFA) [4–6] (for a review of the state-of-the-art see Refs. [7–9]). In this approach, the effect of the laser field on the electron motion after ionization is treated exactly while the effect of the binding potential is neglected. While this approach works well for the electron detachment from (the short-range potential of) negative ions, no justification to disregard the long-range Coulomb interaction in the case of atoms or positive ions exists. Moreover, there are several well-documented features in photoelectron spectra which can hardly be explained within the standard SFA approach. In particular, this includes: (i) orders-in-magnitude enhancement of tunnel ionization rates of atoms and positive ions [8,10,11]; (ii) peculiarities in the extremely-low-energy part of photoelectron momentum distributions [12–16]; (iii) the left-right asymmetry in stereo above-threshold ionization (ATI) setups using carrier-envelope phase-stabilized laser pulses [17].

It is always most intriguing if a pronounced, qualitative effect of the commonly neglected force, i.e., the Coulomb force in our case, can be identified. A possible candidate for an effect of such kind is the violation of the fourfold symmetry of photoelectron angular distributions in elliptically polarized laser light [18–22]. This effect is more robust than the aforementioned left-right asymmetry [17] since it is present also for long pulses with arbitrary carrier-envelope phase. It is also more sensitive to parameters because of the richer kinematics of photoelectrons in elliptically polarized laser fields. Indeed, it was shown that ATI spectra in elliptically polarized fields are particularly sensitive to details of the electron-ion interaction and display effects which remain hidden otherwise [23,24]. While the SFA predicts a fourfold symmetry of the photoelectron distribution for an arbitrarily polarized laser field, the experiments show that in elliptically polarized laser light this symmetry is clearly broken [18,21]. According to the intuitive semiclassical ionization picture [25], which often is in a remarkable agreement with the predictions of the SFA, the most probable photoelectron momentum is along the *minor* polarization axis of the polarization ellipse for intermediate ellipticities, say, $0.2<\xi<0.8$. This effect of classical dodging [23,26] simply follows from the fact that the electron tunnels out with zero velocity at the "tunnel exit" with highest probability near the maximum of the electric field. At that time the vector potential $\mathbf{A}(t)$ is oriented along the minor polarization axis, determining the drift photoelectron momentum $\mathbf{p}=\mathbf{v}-\mathbf{A}$ (atomic units $\hbar=e=m$ are used, the speed of light is included into the definition of the vector potential) measured at a detector. A typical example for a fourfold symmetric angular distribution in polar representation predicted by the SFA is given in Fig. 1. However, the experimental result does not display the fourfold symmetry at all: photoelectrons go predominantly along the major polarization axis and the distribution possesses inversion symmetry only. Remarkably, up to now no satisfactory agreement between theory and experiment [21] has been achieved for this important case. In particular, although the predictions of the Coulomb-Volkov approximation also demonstrate strong violation of fourfold symmetry in the angular distributions [19,20] they were never, to the best of our knowledge, quantitatively compared neither with

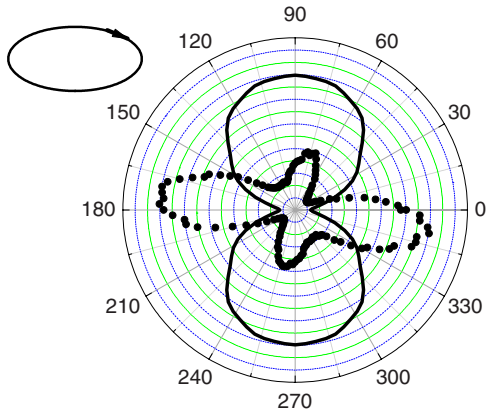

FIG. 1. (Color online) Angular distributions for a photoelectron energy $\epsilon \simeq 2.8$ eV and ionization from the ground state of argon by a Ti:Sa laser ($\lambda = 800$ nm) of intensity $\simeq 10^{14}$ W/cm^2 and ellipticity $\xi = 0.36$. The data recorded in Ref. [21] are shown by dots; the solid line is the SFA prediction. The orientation of the polarization ellipse is shown in the upper left inset with the rotation direction of the electric field vector indicated by an arrow.

the data of Refs. [18,21] nor with *ab initio* results. In Ref. [22], predictions of a simple theory based on a classical account of the Coulomb force acting on the outgoing photoelectron were compared with the data [21]. It was shown that the angular distributions predicted by the theory reproduce the data qualitatively correct, for some ATI peaks even with quantitative accuracy, while for other peaks a significant quantitative disagreement was found. This not only reveals a principle, unsolved problem of strong-field and attosecond laser physics but has direct consequences for novel attosecond pump-probe schemes based on a time-dependent laser polarization, e.g., two-dimensional streaking [27] or the "imaging" of effective atomic potentials.

In recent years new opportunities to examine different theoretical approaches have appeared by *ab initio* numerical solutions of the time-dependent Schrödinger equation (TDSE) for one and two-electron systems driven by strong laser fields [28,29]. Compared to real experiments these numerical experiments provide more stringent tests for analytical theories since all parameters are exactly known and no focal averaging washes out details of the spectra.

In this work, we present an approach to incorporate Coulomb effects into the SFA by accounting for the influence of the Coulomb force on the dominant quantum trajectory of the emitted electron. The method is based on the representation of the SFA in terms of complex trajectories [10,30] or, equivalently, on the imaginary time method [31]. The success of our approach is tested by comparing results to those obtained by numerically solving the time-dependent Schrödinger equation in three spatial dimensions for atomic hydrogen, neon, and argon in elliptically polarized laser fields. The results from these extremely demanding simulations (typical run times $\simeq 20$ days) in turn are compared to the experimental data of Ref. [21]. In addition to justification of the new analytical approach, our *ab initio* calculations show a strong circular dichroism in the high-energy part of ATI spectra.

The paper is organized as follows. In the next section we describe our method for the inclusion of the Coulomb field into the SFA and the *ab initio* numerical solution of the TDSE. Section III is devoted to comparisons between predictions of the standard SFA, the Coulomb-corrected SFA, *ab initio* results, and the data. In the same section the spectra obtained from the TDSE solution are also being analyzed in their high-energy part, where a circular dichroism is found and discussed. The last section is devoted to the conclusions.

II. THEORETICAL APPROACH AND *AB INITIO* CALCULATIONS

A. Coulomb-corrected SFA

We now introduce a Coulomb-corrected version of the SFA (CCSFA) along the ideas proposed in Ref. [10] using the formalism of complex trajectories. Within the SFA the transition amplitude between an atomic bound state $|\Psi_0\rangle$ of binding energy $\epsilon_b \equiv -I$ and a continuum state $|\Psi_{\mathbf{p}}\rangle$ with asymptotic momentum $\mathbf{p}$ is given by

$$M_{\mathrm{SFA}}(\mathbf{p}) = -i\int_{-\infty}^{+\infty} \langle \Psi_{\mathbf{p}}|\hat{V}(t)|\Psi_0\rangle dt, \tag{1}$$

where the final state is approximated by the Volkov function

$$\Psi_{\mathbf{p}}(\mathbf{r},t) = \exp\left\{ i[\mathbf{p}+\mathbf{A}(t)]\cdot\mathbf{r} - \frac{i}{2}\int_{-\infty}^{t} [\mathbf{p}+\mathbf{A}(t')]^2 dt' \right\} \tag{2}$$

and $\hat{V}(t) = \mathbf{E}(t)\cdot\mathbf{r}$ is the interaction operator. The laser field is described by the vector potential $\mathbf{A}(t)$ which depends only on time in the dipole approximation we use here. The electric field is given by $\mathbf{E}(t) = -\partial_t \mathbf{A}$.

It is well-known that the SFA admits a transparent interpretation in terms of complex trajectories, also called quantum orbits [30]. The essence of the complex trajectories method is as follows: for each value of the final photoelectron momentum $\mathbf{p}$ a single or a few complex electron trajectories $\mathbf{r}_0(\mathbf{p},t)$ (per laser period) can be found which satisfy the classical equation of motion for an electron in a laser field

$$\ddot{\mathbf{r}}_0 = \dot{\mathbf{v}}_0 = -\mathbf{E}(t) \tag{3}$$

with the initial and boundary conditions

$$\mathbf{v}_0^2(\mathbf{p}, t = t_s) = -2I, \quad \mathrm{Re}[\mathbf{r}_0(\mathbf{p}, t_s)] = 0,$$

$$\mathbf{v}_0(t \to +\infty) = \mathbf{p} + \mathbf{A}(t \to \infty) = \mathbf{p}. \tag{4}$$

The first two of the conditions (4) imply that the electron begins its motion at the time instant $t_s(\mathbf{p})$ at the origin (where the atom is located) having the kinetic energy equal to the binding energy. According to the third condition the photoelectron appears at a detector with the asymptotic momentum $\mathbf{p}$. The trajectories are classical in the sense that they are solutions of the classical equations of motion but complex, reflecting the fact that tunneling or multiphoton ionization from the ground state of atoms is a quantum effect. Indeed, since the initial electron energy is negative, the initial time $t_s(\mathbf{p})$ must be complex. A respective trajectory is, in general, complex too in complex time but it always becomes real as

soon as time is coming onto the real axis $t \geq t_0(\mathbf{p}) = \mathrm{Re}[t_s(\mathbf{p})]$. The position where the electron appears in real space and time $\mathbf{R}_0(\mathbf{p}) = \mathbf{r}_0[t = t_0(\mathbf{p})]$ is commonly interpreted as the "tunnel exit." In subatomic $E_0 \ll E_{\mathrm{at}} = (2I)^{3/2}$ low-frequency $\omega \ll I$ fields this position is always far from the ion $R_0 \gg 1/\sqrt{2I}$.

With the above-described trajectories the probability amplitude (1) can be represented in the form

$$M_{\mathrm{SFA}}(\mathbf{p}) = \sum_{\alpha} \mathcal{P}_{\alpha}(\mathbf{p}) \frac{\exp[iW_{0\alpha}(\mathbf{p})]}{\sqrt{\partial_t^2 W_{0\alpha}(\mathbf{p})}}, \tag{5}$$

where

$$W_0(\mathbf{p}) = \int_{t_s}^{+\infty} \left(\frac{1}{2}\mathbf{v}_0^2 - \mathbf{E}(t) \cdot \mathbf{r}_0 - I \right) dt - \mathbf{p} \cdot \mathbf{r}_0(+\infty) + \mathbf{v}_0(t_s) \cdot \mathbf{r}_0(t_s) \tag{6}$$

is the classical reduced action evaluated along the complex trajectory and the pre-exponential $\mathcal{P}$ contains the spatial matrix element. If two or more trajectories contribute significantly to Eq. (5), an interference structure appears in the spectrum. Contributions of the respective trajectories are labeled by the subscript α in Eq. (5).

The representation of the SFA in terms of complex trajectories opens up a direct way to include the Coulomb field into the theory. As long as for most of the part of a relevant trajectory the Coulomb force remains small compared to the laser field [this condition is specified by the inequality Eq. (12) below], it can be perturbatively accounted for through corrections to the trajectory $\mathbf{r}_1(\mathbf{p},t)$, to the complex time, and to the action. The latter contains two contributions: one is due to the appearance of the potential energy U_C in the action

$$W_C^{(\mathrm{I})}(\mathbf{p}) = -\int_{t_s(\mathbf{p})}^{+\infty} U_C[\mathbf{r}_0(\mathbf{p},t)]dt = \mathcal{Z}\int_{t_s(\mathbf{p})}^{+\infty} \frac{dt}{|\mathbf{r}_0(\mathbf{p},t)|}, \tag{7}$$

another one is due to the correction $\mathbf{r}_1$ to the trajectory

$$W_C^{(\mathrm{II})}(\mathbf{p}) = \int_{t_s(\mathbf{p})}^{+\infty} [\mathbf{v}_0 \cdot \mathbf{v}_1 - \mathbf{E}(t) \cdot \mathbf{r}_1]dt. \tag{8}$$

The correction $\mathbf{r}_1(\mathbf{p},t)$ has to be determined from the Newton equation

$$\ddot{\mathbf{r}}_1 = -\frac{\mathcal{Z}(\mathbf{r}_0 + \mathbf{r}_1)}{|\mathbf{r}_0 + \mathbf{r}_1|^3}. \tag{9}$$

Here $\mathcal{Z}$ is the residual ion charge; $\mathcal{Z}=1$ for single ionization of a neutral atom.

The above-described procedure is based on the perturbation theory for the action commonly used in quantum and classical mechanics. However, the particular implementation of this method we consider here meets with three essential difficulties:

(i) Corrections (7) and (8) may be logarithmically divergent at the lower integration limit $t \to t_s$ when the electron approaches the nucleus. Here the singular Coulomb force cannot be treated perturbatively.

(ii) A zero-order trajectory $\mathbf{r}_0(\mathbf{p},t)$ may revisit the nucleus in real time (such trajectories are known to be responsible for the rescattering phenomena). This causes another divergence.

(iii) It is unclear which initial conditions should be attached to Eq. (9) for the correction $\mathbf{r}_1(\mathbf{p},t)$.

The problem (i) was solved already in Ref. [10] (see also Refs. [8,32] for detail). It is shown that the divergent part of the Coulomb-induced action can always be matched with the asymptotic of a bound state atomic wave function, and this procedure eliminates a divergency. Moreover, the "sub-barrier" part of the Coulomb corrections, i.e., that part of Eqs. (7) and (8) which accumulates in complex time $t \in [t_s, t_0]$ influences basically the total ionization probability. Therefore, considering the shape of the spectra, we may disregard these "sub-barrier" corrections. In the field with nonzero elliptical polarization where all trajectories are two dimensional, only a very small fraction of them revisit the nucleus, so that the problem (ii) is significant in the field with linear polarization or for small ellipticities. Therefore, in the case of elliptical polarization (we are interested in here) only the problem (iii) is of importance.

According to the argumentation given above we consider trajectories in real time $t \geq t_0$ and assume that they do not approach the ion. If we take a trajectory $\mathbf{r}_0(\mathbf{p},t)$ and evaluate a correction in real time by solving Eq. (9) for $t \geq t_0$ then we obtain a different final photoelectron momentum $\mathbf{v}(t \to +\infty) \neq \mathbf{p}$. This is not what we need for the evaluation of the corrected amplitude for a fixed final momentum $\mathbf{p}$. Instead, let us assume that we know some other Coulomb-free trajectory $\mathbf{r}_0(\tilde{\mathbf{p}},t)$ such that, if we account for the Coulomb force at $t \geq \tilde{t}_0$, the final momentum will exactly have the desired value $\mathbf{p}$. Below we denote such a trajectory $\mathbf{r}_0(\tilde{\mathbf{p}},t) \equiv \tilde{\mathbf{r}}_0(\mathbf{p},t)$. A corresponding stationary point $\tilde{t}_s(\mathbf{p})$ satisfies Eq. (4) with $\tilde{\mathbf{p}}$ instead of $\mathbf{p}$ so that

$$\tilde{t}_s(\mathbf{p}) = t_s(\tilde{\mathbf{p}}). \tag{10}$$

With this new stationary point and the respective new starting points in real time $\tilde{t}_0 = \mathrm{Re}[\tilde{t}_s]$ and space $\tilde{\mathbf{R}}_0 = \mathbf{r}_0(\tilde{\mathbf{p}}, \tilde{t}_0)$ the initial conditions for the Coulomb correction $\mathbf{r}_1$ are: $\mathbf{r}_1(\tilde{t}_0) = \mathbf{v}_1(\tilde{t}_0) = 0$. Now we may find this correction from Eq. (9) and calculate the respective actions (7) and (8). This, however, is even not necessary to do in our case. Indeed, in the approximation we use integration is carried out in real time so that both Eqs. (7) and (8) are real. It is known that for nonzero ellipticities a contribution from one trajectory (per laser period) essentially dominates over that which is from another trajectory, so that no interference appears in the spectrum. Obviously, under such conditions the corrections (7) and (8) only change the phase of the ionization amplitude and have no influence on the spectra.

Summarizing, as far as the shape of photoelectron momentum distributions (but not the total probability) in elliptically polarized fields is concerned, the effect of the Coulomb force can be accounted for via renormalization of the stationary point as prescribed by Eq. (10). Therefore, the corrected ionization amplitude has the form

$$M_{\mathrm{CCSFA}}(\mathbf{p}) = \sum_{\alpha} \mathcal{P}_{\alpha}(\mathbf{p}) \frac{\exp[i\tilde{W}_{0\alpha}(\mathbf{p})]}{\sqrt{\partial_t^2 W_{0\alpha}(\mathbf{p})}}, \tag{11}$$

where $\tilde{W}_0(\mathbf{p})$ is given by Eq. (6) with $\tilde{\mathbf{p}}$ and $\tilde{t}_s$. Since the pre-exponential is a weakly dependent function of the parameters (as compared to the exponential), we neglect corrections to it.

Except some limiting cases the trajectory $\tilde{\mathbf{r}}_0(\mathbf{p},t)$ and the respective stationary point (10) can only be found numerically. Since not the initial but the final condition $\mathbf{v}(t\to+\infty)=\mathbf{p}$ is fixed we have to deal with an inverse problem. In the calculations presented below we solve this inverse problem numerically by iterations taking the Coulomb-free trajectories $\mathbf{r}_0(\mathbf{p},t)$ as a zero-order approximation. Evaluation of one Coulomb-corrected trajectory takes a fraction of a second on a PC using a standard solver for differential equations.

A condition for the applicability of the CCSFA in the above-described formulation can be deduced from the requirement that the absolute value of the Coulomb-induced action must be small compared to the one of the laser-induced action $|W_0(\mathbf{p})|$ and the Coulomb field of the ion near the tunnel exit must be small with respect to the laser field amplitude. These two requirements can be summarized in the inequality

$$1 \gg \frac{E_0}{E_{\mathrm{at}}} \times \begin{cases} 1, & \gamma \ll 1, \\ \gamma^2, & \gamma \gg 1, \end{cases} \tag{12}$$

where $\gamma=\sqrt{2I}\omega/E_0$ is the Keldysh parameter [4] and E_0 is the field amplitude. Condition (12) shows that the standard SFA can only be used as a zeroth-order approximation for the development of a quantitatively correct theory of strong-field ionization in case of relatively weak $E_0 \ll E_{\mathrm{at}}$ and low-frequency $\omega \ll I\sqrt{E_0/E_{\mathrm{at}}}$ laser fields. Beyond this domain, particularly in super-atomic fields, the SFA cannot be expected to provide even a qualitative description, as is known from comparisons with exact numerical results [8,34].

B. *Ab initio* calculations

To examine the theory introduced above we perform exact numerical solution of the TDSE for a model single active electron atom in an elliptically polarized field. A detailed description of the numerical method is given in Ref. [28].

We consider an atom with a single active electron whose bound state wave function of energy $\epsilon_{bl}\equiv -I$ can be written as $\Psi(\mathbf{r})=\Phi(r)Y_{lm}(\vartheta,\varphi)$ with $\Phi(r)$ the radial wave function and l,m the orbital and magnetic quantum number, respectively. We either constructed the self-consistent effective potential $U(r)$ using ground-state density functional theory [33] or approximated it by a screened Coulomb potential (leading to very similar results) $U(r)=-[1+(z-1)e^{-\kappa r}]/r$ where z is the nuclear charge (e.g., $z=18$ for argon) and κ is chosen to adjust the value of the binding energy ϵ_{bl}. The pulse with the carrier frequency ω ($\lambda=800$ nm), amplitude E_0, ellipticity ξ and a duration of $n=8$ optical cycles polarized in the (x,y) plane is described by the vector potential

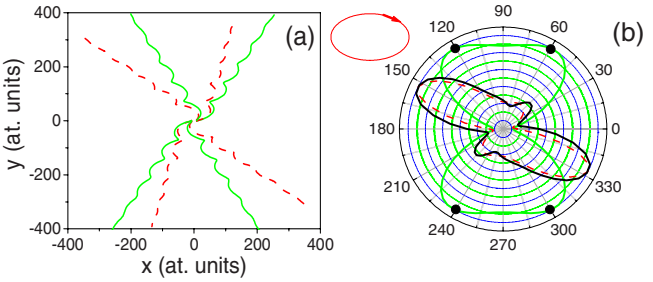

FIG. 2. (Color online) Rotation of electron trajectories (a) and AD (b) for ionization from the ground state of hydrogen by the field (13) with intensity 10^{14} W/cm^2, $\xi=0.5$, $\hbar\omega=1.55$ eV, and photoelectron energy $\epsilon=7.9$ eV. Panel (a) shows four classical electron trajectories with Coulomb interaction neglected (green solid) for emission angles 60°, 120°, 240°, and 300° [black circles in the SFA AD, panel (b)]. The Coulomb-corrected trajectories and AD are also shown (red dashed). In (b) the *ab initio* TDSE result is plotted black.

$$\mathbf{A}(t) = A_0\left[\sin^2\left(\frac{\varphi}{2n}\right)\cos\varphi, -\xi\sin^2\left(\frac{\varphi'}{2n}\right)\cos\varphi'\right] \tag{13}$$

with $A_0=E_0/(\omega\sqrt{1+\xi^2})$, $\varphi\equiv\omega t$, $\varphi'=\varphi-\pi/2$, and $0\le\varphi,\varphi'\le 2\pi n$.

III. RESULTS AND DISCUSSION

We calculate angular distributions (ADs) for a given ATI maximum

$$\frac{dW}{d\phi} \sim p_s|M(\mathbf{p}=p_s\mathbf{n})|^2, \tag{14}$$

where $p_s=\sqrt{2\epsilon_s}$, $\epsilon_s=s\omega-I-U_P$ is the absolute value of the photoelectron final momentum in the sth ATI maximum of energy ϵ_s, and $\mathbf{n}$ and ϕ are the unit vector and the azimuthal angle in the polarization plane, respectively. For the field (13) the ponderomotive energy $U_P=E_0^2/4\omega^2$ is ellipticity independent. The amplitude $M(\mathbf{p})$ in Eq. (14) is given by Eq. (1) for the standard SFA and by Eq. (11) for its Coulomb-corrected version.

A. Low-energy electrons: Coulomb distortion of trajectories

To test the theory we start from the simplest case of hydrogen. The main physical effect whose consequences we expect to find in the AD is the Coulomb distortion of trajectories which breaks the fourfold symmetry. Figure 2(a) shows four Coulomb-free trajectories (green solid) corresponding to four emission directions symmetrical with respect to the major and the minor polarization axes. Obviously, the SFA ionization probabilities are exactly equal to each other for these emission angles. The four red dashed trajectories are the full solutions of Eq. (9) with the same initial conditions as for the respective Coulomb-free trajectories. One may observe that each Coulomb-corrected trajectory not only rotates about the origin but the electron also accelerates or decelerates as compared to the unperturbed trajectory, giving rise to a complicated deformation of the

spectra. It is important to note that such huge qualitative changes are induced by a small perturbation. In fact, for the parameters of Fig. 2 the initial radius for each trajectory is $|\mathbf{R}_0| \simeq 8$ a.u., where the magnitude of the Coulomb force is $F_C = 1/R_0^2 \simeq 0.016$ a.u., i.e., about three times less than the laser force amplitude. The physical reason why the Coulomb effects appear to be significant even in the perturbative regime is that the Coulomb force acts constantly in addition to the oscillating laser force and therefore affects the electron dynamics in an accumulative manner. According to the explanations given in the previous section, instead of the trajectories shown in Fig. 2(a) which, after accounting for the Coulomb force, lead to the states with different final momenta, we should find other trajectories $\tilde{\mathbf{r}}$ and the respective new initial conditions and stationary points to provide the same value of the final momenta. We do not show these trajectories in Fig. 2(a) since they asymptotically coincide with the initial Coulomb-free trajectories and differ from them only near the starting point because of different initial conditions.

In Fig. 2(b) we compare the AD resulting from the above-described CCSFA approach with the prediction of the standard SFA and the *ab initio* result. It is seen that the influence of the Coulomb field leads to a pronounced effect in the AD. A very good qualitative agreement between the CCSFA and the TDSE result gives a strong support to the idea that the asymptotic Coulomb force is mainly responsible for disagreements between predictions of the SFA and exact results.

In Fig. 3 we show more comparisons with *ab initio* results for different photoelectron energies, intensities, and different atoms. These comparisons show that the CCSFA approach also works for complex atoms with the electron initially in a state of nonzero angular momentum. For neon we show also the *ab initio* result for partial AD with respect to states of magnetic quantum number $m = \pm 1$ within the p-shell. The quantization axis is perpendicular to the plane of polarization, so that the contribution from the state with $m=0$ is negligibly small. Only in Fig. 3(c) the agreement is not satisfactory because of the low ATI energy. For the parameters of Figs. 2 and 3 the value (12) is varying within the interval $0.04-0.1$, so that the perturbative approach we use for the inclusion of the Coulomb force is well justified, and the CCSFA gives almost exact results. The standard SFA with its fourfold symmetry is in strong disagreement with both CCSFA and numerical TDSE results. The latter two display inversion symmetry only and a rotation of the distribution maximum toward the major polarization axis. This rotation is especially pronounced for the low-order peaks.

In Fig. 4 we compare our *ab initio* results with the data for argon recorded in the experiment [21]. Although, the calculation reproduces the data quite well (while the standard SFA does not reproduce them at all), the quantitative agreement is not so good as it is between CCSFA and TDSE results. Moreover, to improve the agreement with respect to the positions of the AD maxima the TDSE simulation was performed for an intensity 0.6×10^{14} W/cm^2, which is approximately $1.3-1.5$ times less than the one declared in the experiment [21]. The disagreements between the experiment and the theory may be attributed to uncertainty in the experimental parameters and the focal averaging effect or to the influence of the atomic structure, which is modeled in our numerical TDSE calculation only in a very simple way.

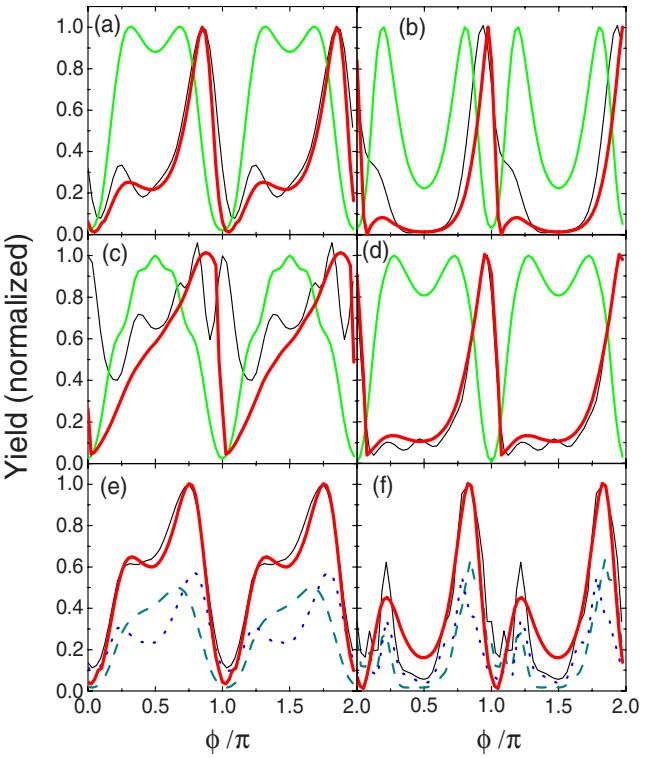

FIG. 3. (Color online) Comparison of the CCSFA (bold red) with the results of the *ab initio* TDSE solution (thin black) for the parameters (a),(b) of Fig. 2 for hydrogen, (c),(d) for argon at intensity 0.6×10^{14} W/cm^2 and ellipticity $\xi=0.36$, and (e),(f) for neon at intensity 2×10^{14} W/cm^2 and ellipticity $\xi=0.36$. The photoelectron energies are 8.2 eV (a), 12.8 eV (b), 1.4 eV (c), 4.6 eV (d), 7.1 eV (e), and 11.7 eV (f). The standard SFA prediction is included in plots (a)–(d) (green solid). For argon and neon the ionization probability is averaged over the magnetic quantum numbers $m=0,\pm1$ within the p shell. For neon (e),(f) the contributions from the state with $m=1$ and $m=-1$ are also shown (cyan dashed and blue dotted, respectively) while the SFA contribution is omitted.

B. High-energy electrons: strong circular dichroism in rescattering

Upon a change of the sign of ellipticity ($\xi\rightarrow-\xi$) the distributions reflect with respect to any of the polarization axes. This is a manifestation of elliptical dichroism (ED), well-studied for negative ions [35] and, in low-intensity fields, for atoms [36]. From the results given above we deduce that the Coulomb interaction is the physical reason behind the ED in the strong-field ionization of atoms. This explains also why for negative ions ED remains a relatively weak effect.

In addition to the ED, which does not affect the angle-integrated probability, examination of our results shows also the presence of circular dichroism (CD). The last appears in the AD with a fixed value of m of the initial state [see blue dotted and cyan dashed curves in Figs. 3(e) and 3(f)]. In addition to the property $W(\phi,\xi)=W(\pi-\phi,-\xi)$ of the m-averaged AD [which is obviously also satisfied for

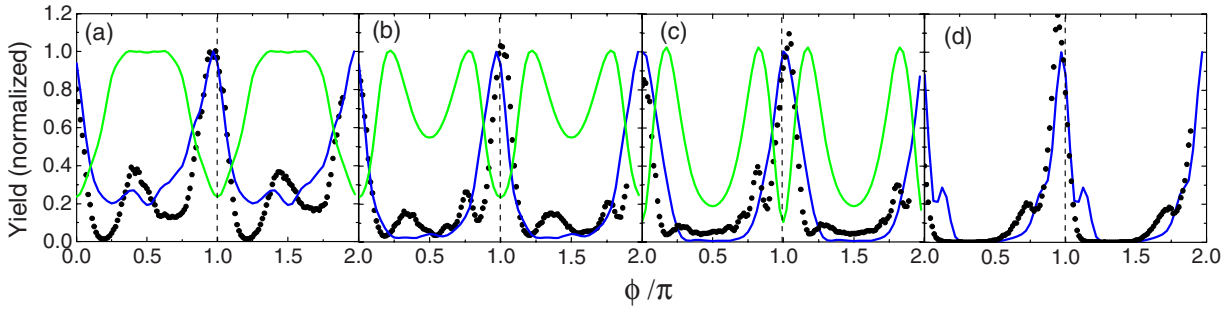

FIG. 4. (Color online) Normalized angular distributions in the polarization plane ($\xi=0.36$) for argon and photoelectron energies 2.8 eV (a), 6.0 eV (b), 9.2 eV (c), and 21.8 eV (d). Experimental data (black filled circles), TDSE calculation (blue solid), plain SFA (green solid). The laser intensity was assumed 0.6×10^{14} W/cm^2, the laser wavelength $\lambda=800$ nm. The photoelectron energy in (d) lies already in the rescattering plateau so that the plain SFA prediction is omitted. The major polarization axis corresponds to $\phi=0,\pi$.

$W_m(\phi,\xi)$] we now have $W_m(\xi)=W_{-m}(-\xi)\neq W_m(-\xi)$, where $W_m(\xi)$ is the angle-integrated probability. It is interesting that while in the low-energy part of the spectrum this dichroism remains a small effect in the sense that W_m and W_{-m} are of the same order of magnitude, in the high-energy plateau the difference in the angle-integrated probabilities is quite pronounced, even for a rather low ellipticity $\xi=0.36$ and can be several orders of magnitude for higher charge states. This difference between the low-energy domain and the rescattering plateau is clearly visible from the angle-integrated spectra shown in Fig. 5. The degree of CD can also be characterized by the energy-dependent dichroism parameter

$$\delta(\epsilon)=\frac{W_{-1}-W_{+1}}{W_{-1}+W_{+1}} \tag{15}$$

shown in the inset of Fig. 5. The state with $m=-1$ contributes to rescattering much stronger than the one with $m=1$ (the small contribution from the state with $m=0$ is not shown).

A strong CD in the plateau domain can be explained using simple semiclassical arguments in the spirit of the simple man's ionization model [37]. Electrons liberated from the atom populate initially the low-energy part of ATI spectrum

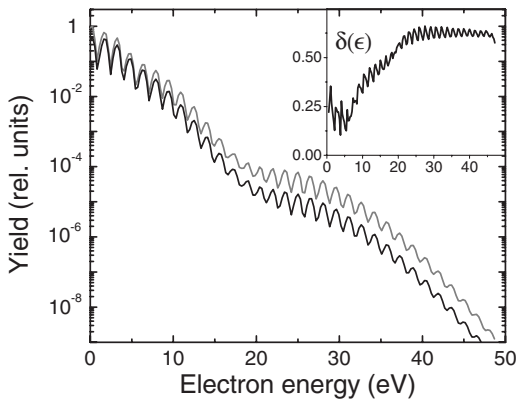

FIG. 5. Angle-integrated photoelectron spectra obtained from the TDSE solution for argon, parameters of Figs. 3 and 4. Contributions from the states $m=1$ and $m=-1$ are shown black and gray, respectively. The dichroism parameter (15) vs the photoelectron energy ϵ is shown in the inset.

up to $2U_P$. If they move on to the detector without a hard recollision they remain low-energetic and their energy distributions experience the Coulomb distortion described in the previous subsection. However, being driven back to the origin by the laser field electrons may rescatter at the parent ion into the domain of the high-energy plateau. The precondition for rescattering is the electron's return to the origin, which is possible in a linearly polarized field only where the electrons move mainly along the polarization direction. In a field of elliptical polarization, the electron kinematics become two dimensional. In order to return to the origin the electron should be emitted with a momentum predominantly directed along the main polarization axis [24,38]. It is seen from Fig. 3 that the AD have a minimum for momenta close to the major axis ($\phi\simeq0,\pi$), which is the reason why the rescattering is strongly suppressed with increasing ellipticity. However, for the $m=-1$ initial state the probability for the electron to be emitted with momentum along the major polarization axis significantly exceeds the probability for $m=1$ [see Fig. 3(e)]. Note that in the velocity gauge version of the SFA AD do not depend on the magnetic quantum number at all. Hence the velocity gauge SFA would lead to incorrect results (see, e.g., the discussion of the SFA gauge dependence in Ref. [39]). For rare gas atoms, having a closed shell, a strong CD in the plateau domain is obviously not observable. Its observation would require an atom with no more than four electrons in a p shell, polarized by an external magnetic field prior to the interaction with the laser pulse.

IV. CONCLUSIONS

In conclusion, we introduced a Coulomb-corrected SFA (CCSFA) based on the perturbative account of the long-range Coulomb field of the parent ion and its effect on the classical complex electron trajectories which enter the semiclassical ionization amplitude. For the case of elliptical polarization we showed that the CCSFA yields quantitative agreement with the results from the *ab initio* solution of the time-dependent Schrödinger equation while the standard SFA fails even qualitatively. Although we restricted ourselves to elliptical polarization in this work, we consider the proposed method to be a general improvement of the SFA. In particular it should be applicable to linear polarization where

Coulomb-modified interference of quantum trajectories comes into play. The full description of the theory, including the regularization procedure of the divergent "subbarrier" contributions, a solution of the problem (ii) and application to the case of linear polarization will be published separately [40].

Recently two new generalizations of the Volkov wave function were proposed, namely, the Coulomb-phase-distorted wave function [41] and the eikonal-like approximation for one- and two-electron Coulomb-Volkov continua [42,43]. Both methods are based on a Coulomb correction to continuum wave functions. This type of correction to the wave function corresponds to the evaluation of an infinite number of trajectories covering the whole position space, including the Coulomb singularity at the origin. Obviously, a proper realization of this task in full dimensionality seems to be very demanding. In our approach, only one or a few Coulomb-corrected classical trajectories must be evaluated for each value of the final momentum. On the other hand, the method proposed in Ref. [43] permits one to trace subcycle ionization dynamics, which cannot be achieved within our approach.

ACKNOWLEDGMENTS

We are grateful to W. Becker, S. P. Goreslavski, N. L. Manakov, V. D. Mur, V. S. Popov, and N. I. Shvetsov-Shilovski for valuable discussions. The work was supported by the Deutsche Forschungsgemeinschaft (S.V.P. and D.B.), the Welch Foundation A-1562 (G.G.P.), NSF (G.G.P.), and the Russian Foundation for Basic Research (S.V.P.).

[1] V. L. B. de Jesus, A. Rudenko, B. Feuerstein, K. Zrost, C. D. Schröter, R. Moshammer, and J. Ullrich, J. Electron Spectrosc. Relat. Phenom. **141**, 127 (2004).
[2] D. B. Milošević, G. G. Paulus, D. Bauer, and W. Becker, J. Phys. B **39**, R203 (2006).
[3] P. Agostini and L. F. DiMauro, Rep. Prog. Phys. **67**, 813 (2004).
[4] L. V. Keldysh, Zh. Eksp. Teor. Fiz. **47**, 1945 (1964) [Sov. Phys. JETP **25**, 1307 (1964)].
[5] F. H. M. Faisal, J. Phys. B **6**, L89 (1973).
[6] H.R. Reiss, Phys. Rev. A **22**, 1786 (1980).
[7] W. Becker, F. Grasbon, R. Kopold, D. B. Milošević, G. G. Paulus, and H. Walther, Adv. At., Mol., Opt. Phys. **48**, 35 (2002).
[8] V. S. Popov, Phys. Usp. **47**, 855 (2004).
[9] A. Becker and F. H. M. Faisal, J. Phys. B **38**, R1 (2005).
[10] A. M. Perelomov and V. S. Popov, Sov. Phys. JETP **25**, 336 (1967).
[11] S. L. Chin, C. Rolland, P. B. Corkum, and P. Kelly, Phys. Rev. Lett. **61**, 153 (1988).
[12] J. Chen and C. H. Nam, Phys. Rev. A **66**, 053415 (2002).
[13] R. Moshammer *et al.*, Phys. Rev. Lett. **91**, 113002 (2003).
[14] K.I. Dimitriou, D.G. Arbó, S. Yoshida, E. Persson, and J. Burgdörfer, Phys. Rev. A **70**, 061401(R) (2004).
[15] A. Rudenko *et al.*, J. Phys. B **38**, L191 (2005).
[16] A. S. Alnaser, C. M. Maharjan, P. Wang, and I. V. Litvinyuk, J. Phys. B **39**, L323 (2006).
[17] S. Chelkowski and A. D. Bandrauk, Phys. Rev. A **71**, 053815 (2005).
[18] M. Bashkansky, P. H. Bucksbaum, and D. W. Schumacher, Phys. Rev. Lett. **60**, 2458 (1988).
[19] S. Basile, F. Trombetta, and G. Ferrante, Phys. Rev. Lett. **61**, 2435 (1988).
[20] A. Jaroń, J. Z. Kaminski, and F. Ehlotzky, Opt. Commun. **163**, 115 (1999).
[21] G. G. Paulus, F. Grasbon, A. Dreischuh, H. Walther, R. Kopold, and W. Becker, Phys. Rev. Lett. **84**, 3791 (2000).
[22] S. P. Goreslavski, G. G. Paulus, S. V. Popruzhenko, and N. I. Shvetsov-Shilovski, Phys. Rev. Lett. **93**, 233002 (2004).
[23] G. G. Paulus, F. Zacher, H. Walther, A. Lohr, W. Becker, and M. Kleber, Phys. Rev. Lett. **80**, 484 (1998).
[24] R. Kopold, D. B. Milošević, and W. Becker, Phys. Rev. Lett. **84**, 3831 (2000).
[25] P. B. Corkum, N. H. Burnett, and F. Brunel, Phys. Rev. Lett. **62**, 1259 (1989).
[26] A. M. Perelomov, V. S. Popov, and M. V. Terent'ev, Sov. Phys. JETP **24**, 207 (1967).
[27] S. V. Popruzhenko, N. I. Shvetsov-Shilovski, S. P. Goreslavski, W. Becker, and G. G. Paulus, Opt. Lett. **32**, 1372 (2007).
[28] D. Bauer and P. Koval, Comput. Phys. Commun. **174**, 396 (2006).
[29] C. Ruiz, L. Plaja, L. Roso, and A. Becker, Phys. Rev. Lett. **96**, 053001 (2006).
[30] P. Salières *et al.*, Science **292**, 902 (2001).
[31] V. S. Popov, Phys. At. Nucl. **68**, 686 (2005).
[32] V. S. Popov, V. D. Mur, and S. V. Popruzhenko, JETP Lett. **85**, 223 (2007).
[33] R. M. Dreizler and E. K. U. Gross, *Density Functional Theory. An Approach to the Quantum Many-Body Problem* (Springer, Berlin, 1999).
[34] D. Bauer and P. Mulser, Phys. Rev. A **59**, 569 (1999).
[35] N. L. Manakov, M. V. Frolov, B. A. Borca, and A. F. Starace, J. Phys. B **36**, R49 (2003).
[36] N. L. Manakov, A. Maquet, S. I. Marmo, V. Veniard, and G. Ferrante, J. Phys. B **32**, 3747 (1999).
[37] P. B. Corkum, Phys. Rev. Lett. **71**, 1994 (1993).
[38] S. P. Goreslavski, S. V. Popruzhenko, and N. I. Shvetsov-Shilovski, Laser Phys. **13**, 1054 (2003).
[39] D. Bauer, D. B. Milošević, and W. Becker, Phys. Rev. A **72**, 023415 (2005).
[40] S. V. Popruzhenko and D. Bauer, J. Mod. Opt. (to be published).
[41] F. H. M. Faisal and G. Schlegel, J. Phys. B **38**, L223 (2005); J. Mod. Opt. **53**, 207 (2006).
[42] O. Smirnova, M. Spanner, and M. Ivanov, J. Phys. B **39**, S307 (2006); **39**, S323 (2006).
[43] O. Smirnova, M. Spanner, and M. Ivanov, Phys. Rev. A **77**, 033407 (2008).